Zirconia transformation in multi-phases ceramic composites

ARTICLE *in* JOURNAL OF THE AUSTRALIAN CERAMIC SOCIETY · JANUARY 2015

Impact Factor: 0.66

4 AUTHORS, INCLUDING:

H. Makri

Université de M'sila

4 PUBLICATIONS **1** CITATION

SEE PROFILE

H. Belhouchet

Université de M'sila

16 PUBLICATIONS **28** CITATIONS

SEE PROFILE

Hamidouche Mohamed

Ferhat Abbas University of Setif

56 PUBLICATIONS **251** CITATIONS

SEE PROFILE

Zirconia transformation in multi-phases ceramic composites

H. Makri[1,3], H. Belhouchet[2,3*], M. Hamidouche[4] and G. Fantozzi[5]

1) Département de Génie Mécanique, Faculté de Technologie, Université Mohamed Boudiaf-M'sila, M'sila, 28000, Algérie.
2) Département de physique, Faculté des Sciences, Université Mohamed Boudiaf-M'sila, M'sila, 28000, Algérie.
3) Laboratoire des Matériaux Non Métalliques, I. O. M. P., Université Ferhat Abbas-Sétif 1, Sétif, 19000, Algérie.
4) Unité de Recherche Matériaux Emergents, Université Ferhat Abbas-Sétif 1, Sétif, 19000, Algérie.
5) Université de Lyon, INSA-Lyon, MATEIS CNRS-UMR 5510, 69621 Villeurbanne, France.

Email: hbelhou@yahoo.com

Available Online at: www.austceram.com/ACS-Journal

Abstract
Low cost composite ceramics based on zircon-mullite-zirconia-alumina phases were prepared by reaction sintering of boehmite (AlOOH) and zircon ($ZrSiO_4$) powders. Boehmite to zircon weight ratios of the starting powders were varied (10 to 90 wt. %). The green compacts were made by uniaxial pressing at 7 MPa followed by cold isostatic pressing at 250 MPa. A reactive sintering in air of these compacts was made at different temperatures between 1400 and 1600°C during 2 hours. A quantitative evaluation of the present phases was based on XRD. Dilatometric tests on the reaction-sintered composites were carried out in order to study the zirconia phase's transformations and their thermal expansion coefficient (α). In addition, the effects of both boehmite/zircon ratios and sintering conditions on the mechanical properties (Hardness Hv, Elastic modulus E and fracture toughness K_{IC}) of the obtained composites were characterized by Vickers indentation.

Key words: Multiphase composites, Reaction sintering, Zircon, Alumina, Mullite, Zirconia.

INTRODUCTION

It is generally accepted that ceramics can be toughened by incorporating a dispersed second phase [1]. The addition of zircon in the alumina system has been studied by Claussen et al. [2]. This is an easy and inexpensive route for obtaining a homogeneous ceramic with improved mechanical properties [1]. Usually, zirconia particles are used as a reinforcing addition in ceramic composites [2-4]. Different toughening mechanisms are involved in ceramics composites, (micro-cracking, stress-induced transformation, crack deflection e.t.c) [5-6]. The phase ratio is one of the most important variables [7]. At high temperatures, zircon dissociates in solid state, forming zirconia and amorphous silica [8]. The zircon's decomposition temperature can be decreased by the presence of impurities in the starting powders. The presence of mullite increases the zircon thermal dissociation [9]. The ZrO_2 presence has an influence on the mechanical and fracture properties of these materials through several combined mechanisms [7]. Glassy phases initiating at some triple junctions at high temperatures can however reduce the strength of zircon at these temperatures [9].

The monoclinic-tetragonal (m↔t) transformation of zirconia is considered to be martensitic and occurs at about 1170°C. Under an applied stress, the metastable t-ZrO_2 may spontaneously transform into m-ZrO_2 and absorbs energy [10].

Several of the toughening mechanisms related to martensitic transformation (from tetragonal to monoclinic) explain why zirconia is included into various ceramics matrices as a toughening agent [11]. The toughening and concomitant strengthening have been attributed to the volume and shape changes associated with the stress induced by t↔m transformation, which occurs in the stress field of propagating cracks [12]. However, very few careful studies of the process and mechanisms of the t↔m transformation have been reported because the martensitic transformation is usually too rapid to be clearly observed [10]. Information on the martensitic transformation can be retrieved from thermal expansion measurements using a dilatometer. It enables a real time monitoring of the transformations evolution in terms of dimensional changes occurring in the sample during a thermal cycle. The Dilatometric data can indicate the retained t-phase amount for a pursued toughness enhancement [13]. In cases of mullite-zirconia composite obtained by reacted sintering, temperatures of m→t and t→m transformations were found respectively at 1100 and

 ISSN 0004-881X

785°C by Hamidouche et al. [14]. In a recent work on mullite-zirconia ceramics [15], these transformation temperatures were respectively in the ranges of 1127-1207°C and 977-1052°C. When zirconia is dispersed in a ceramic matrix, the transformation occurs in a range of temperatures depending on the matrix stiffness which is influenced by the incorporated zirconia particle size [16]. The transformation temperature decreases when the zirconia content decreases, which is associated with a decrease in the particle size and an increase in the mechanical constraint due to the matrix. As usual, the t→m transformation of zirconia exhibits a hysteresis behavior and is accompanied by a volume increase of 5%. The area of the hysteresis cycle depends on the fraction of zirconia transformed [17], and can be linked with the m-ZrO_2 content which is measured by the XRD-Rietveld method. The hysteresis can therefore be used to know the m-ZrO_2 amount present in the composite [15].

To quantify ZrO_2 phases presents in the composites products, by XRD analysis, Garvie and Nicholson [18] proposed their equation (1) for estimating and drawing the quantity of tetragonal ZrO_2 present in function of the ratio of the intensity of the tetragonal peaks (111) and of the monoclinic peaks (111) and ($11\bar{1}$). The fraction of the monoclinic phase in the sample is given by the following relation:

$$x_m = \frac{I_m(111)+I_m(11\bar{1})}{I_m(111)+I_m(11\bar{1})+I_t(111)} \qquad (1)$$

where I is the polymorphic intensity of tetragonal or monoclinic zirconia.
Li and Khor [19] reported the phases (R_{ZrO2}, R_{ZrSiO4}, and $R_{mullite}$) by comparing the areas of the peaks of these phases using the following equations:

$$R_{ZrO2(t+m)} = \frac{I_{\{ZrO2-t(111)\}}+I_{\{ZrO2-m(11\bar{1})\}}}{I_{\{ZrSiO4(200)\}}+I_{\{ZrO2-t(111)\}}+I_{\{ZrO2-m(11\bar{1})\}}} X100\% \qquad (2)$$

$$R_{ZrSiO4} = \frac{I_{\{ZrSiO4(200)\}}}{I_{\{ZrSiO4(200)\}}+I_{\{ZrO2-t(111)\}}+I_{\{ZrO2-m(11\bar{1})\}}} X100\% \qquad (3)$$

$$R_{m-ZrO2} = \frac{I_{\{ZrO2-t(111)\}}+I_{\{ZrO2-m(11\bar{1})\}}}{I_{\{ZrSiO4(200)\}}+I_{\{ZrO2-t(111)\}}+I_{\{ZrO2-m(11\bar{1})\}}} X100\% \qquad (4)$$

$$R_{t-ZrO2} = \frac{I_{\{ZrO2-t(111)\}}}{I_{\{ZrO2-t(111)\}}+I_{\{ZrO2-m(111)\}}+I_{\{ZrO2-m(11\bar{1})\}}} X100\% \qquad (5)$$

$$R_{mullite} = \frac{I_{\{mull(210)\}}}{I_{\{ZrSiO4(200)\}}+I_{\{Al2O3(012)\}}+I_{\{mull(210)\}}} X100\% \qquad (6)$$

$$R_{Alumina} = \frac{I_{\{Al2O3(012)\}}}{I_{\{ZrSiO4(200)\}}+I_{\{Al2O3(012)\}}+I_{\{mull(210)\}}} X100\% \qquad (7)$$

I_{Al2O3}, I_{ZrSiO4}, $I_{t\text{-}ZrO2}$, $I_{m\text{-}ZrO2}$, and $I_{mullite}$ are the integrated intensities of sector of Al_2O_3, $ZrSiO_4$, t-ZrO_2, m-ZrO_2 and mullite peaks, respectively. Schmid [20], Leatherman et al. [21] and Zhong et al. [11] used the following relation (equation 8) to determine the relative amounts of tetragonal and monoclinic zirconia:

$$V_m = \frac{1.311\ X_m}{1+0.311\ X_m} \text{ and } Vt = 1 - Vm \qquad (8)$$

Vm and Vt are the volume fraction of monoclinic and tetragonal zirconia respectively. The molar fraction of the zirconia monoclinic Xm is defined as

$$X_m = \frac{[I_m(111)+I_m(11\bar{1})]}{[I_m(111)+I_m(11\bar{1})+I_t(111)]} X100\% \qquad (9)$$

In several works on ceramic composites, in which mullite was the major phase where strengthening was carried out by the incorporation of zirconia as second phase, the authors have used laboratory expensive powders of high purity that require high sintering temperatures [8, 22-25]. Moreover, the grinding process for these powders takes a long time and sometimes degrades the grinding material (balls and pot). In some cases, the preparation protocol is complex requiring special precautions [26-27].

The purpose of this work was to study the dilatometric behavior of the Zircon-mullite-zirconia--alumina multiphase composites obtained by reaction sintering on the basis of only two starting powders (boehmite and zircon). The boehmite powder (for α-alumina replacement) was used to decrease the processing cost. A quantitative study of the phases present was also performed to correlate the behavior with the phase composition and the ZrO_2 critical quantity affecting the apparition of hysteresis in the dilatometric curves.

METHODS AND PROCEDURES

2.1 Materials used

Two commercial raw materials were used to obtain multiphase composites materials:

1) Boehmite powder (noted B) was used as alumina source, obtained from partial dehydration of a commercial gibbsite powder (supplied by Diprochim, Algeria). The average particle size of this powder is 75 μm.

2) A fine zircon powder (noted ZS), supplied by Moulin des Près (France Company), with 1.5 μm of average particle size.

The boehmite powder was milled by attrition with alumina balls in aqueous media for 3 h to reduce D_{50} to 1.5 μm. Milling was carried out under the following conditions: the powder to ball ratio was kept to 1:10 by weight. Suspensions at pH 10.4 were prepared by adding ammoniac and approximately of 0.25 wt.% of ammonium polymethacrylate dispersant (Darvan C). Homogenization of the mixtures of boehmite and zircon was achieved by ball-milling for 20 hours in distilled water using alumina balls of

diameters within the range (1.5-2 mm) and a plastic container under the same preceding conditions. After milling, the mixtures were dried at 110°C during 2 hours. As binder, we added by mortar mixing, 1 wt.% of polyvinyl alcohol (PVA) and 0.5 wt.% of polyethylene glycol (PEG). The mixtures were then granulated through a 45 µm sieve.

Samples shaped as disks (diameter: 15 mm) with different percentages of boehmite to zircon weight ratios from 10 to 90 wt.%. The samples were compacted by uniaxial pressing at 7 MPa followed by cold isostatic pressing at 250 MPa. They were heated up to 600°C at a rate of 1°C/min to burn out the binder. Finally were sintered in air between 1400 and 1600°C for 2 hours using a heating rate of 5°C/min.

2.2 Characterization techniques

Crystalline phases formed of sintered composites were identified by X-ray diffraction (XRD) using a Rigaku diffractometer [using Ni-filtered Cuk_α radiation (40kV-25mA) with a scanning speed (2θ) of 2° per minute and 0.05° of step]. On the basis of the peaks areas corresponding to (111) and $(11\bar{1})$ of monoclinic zirconia, (111) of tetragonal zirconia, (200) of zircon, (113) of α-alumina and (110) of mullite, a quantitative analysis was carried out to estimate the fraction of dissociated zircon, alumina, mullite formation and the bulk retained of m and t-ZrO_2 on the sintered samples polished surfaces using methods found in literature [18-20, 28-29]. Linear thermal expansion was performed between the ambient and 1400°C with 5°C/min heating rate on the cylindrical sintered rods (10 mm of length and 10 mm of diameter) using a NETZSCH dil 402C dilatometer. The curves obtained were analyzed to study the Zt/Zm and Zm/Zt phase transformations of the zirconia among the multiphasic composites. A scanning electron microscopy was obtained on the polished surface of a thermally etched sample using SEM (JEOL-840-A). Instrumented indentation was used for evaluating Vickers hardness and elastic modulus. The tests were performed on a Zwick Roell ZHU2.5 testing machine using the following conditions: a 15 N loading charge, 15 s dwelling time and a loading rate of 0.5 mm / min and a discharge Rate of 0.1 mm / min. The fracture toughness was determined by indentation, using the radial cracks which appear at the corner of the Vickers imprint. The K_{IC} was evaluated according to Anstis et al. relation [30-31]:

$$K_{IC} = 0{,}016\left(\frac{E}{H}\right)^{\frac{1}{2}}\left(\frac{p}{C^{\frac{3}{2}}}\right) \quad (10)$$

E: the elastic modulus, H: the hardness, P: the indentation load, C: the radial crack length.

RESULTS AND DISCUSSION

3.1 Phase's identification

Figure 1 shows the XRD patterns of the various composites sintered at 1600°C during 2 hours. An emergence of zircon peaks, with small peaks of mullite for composites of 10 wt.% of boehmite (zircon-mullite composites was formed). In the case of b and c spectra, the intensity of mullite peaks increases with increasing boehmite addition. Interestingly, the formed zirconia appears in both monoclinic and tetragonal phases. Zircon-mullite-zirconia composites are then obtained. The same situation was observed for a ratio of 40 wt.% of boehmite where mullite-zircon-zirconia composites were formed. Fig. 1-e and 1-f shows enrichment by zirconia and mullite as a consequence to the zircon's dissociation. The formation of mullite uses all the alumina quantity eminent from the boehmite transformation, and all SiO_2 obtained from zircon's dissociation. Mullite-zirconia composites are obtained in the samples containing 50 and 60 wt.% of boehmite.

Figures 1-g and 1-h show a case of insufficiency of zircon. Mullite was formed in quantities proportional to the small quantity of SiO_2 from zircon dissociation. The presence of high amount of alumina in the samples containing 70 and 90 wt.% of boehmite favours the formation of t-zirconia. The mullite-zirconia-alumina and alumina-mullite-zirconia composites were formed in the samples containing respectively 70 and 90 wt.% of boehmite. Mullite-zirconia composites were formed in the samples containing 50 and 60 wt.% of boehmite. In the lower parts of these percentages of boehmite (zircon is in excess), we obtain the composites of zircon-mullite and zircon-mullite-zirconia. When alumina is in excess, composites of mullite-zirconia-alumina and alumina-mullite-zirconia were obtained.

3.2 Dilatometric Study

We collected the dilatometric results for all composites obtained from the different ratios of starting powders and sintered at 1600°C (Fig. 2). In the case of zircon-mullite (ZSM) and zircon-mullite-zirconia (ZSMZ) composites, due to low starting boehmite (≤ 20 wt.%) and alumina-mullite-zirconia (AMZ) composites, obtained from a high level of boehmite (≥ 90 wt.%), the curves are almost linear. When the level of starting powders of boehmite are between 30 and 70 wt.% (mullite-zirconia composites) the curves exhibit reversible hysteresis. This phenomenon is characteristic of the reversible phase transformation of zirconia ($t \leftrightarrow m$) observed in others works (Hamidouche et al. [14] and Basu et al. [13]). In general, this transformation occurred at around 1100°C during heating and at about 785°C during cooling [14]. The hysteresis area for the zircon-mullite-zirconia (ZSMZ) composites, due to low starting boehmite dosage, is very small. The formation mechanism of the mullite phase in these composites is by precipitation from a glassy phase containing dissolved alumina in accordance to the reference [32]. The regions where the zirconia grains are localized are richer in amorphous silica phase and

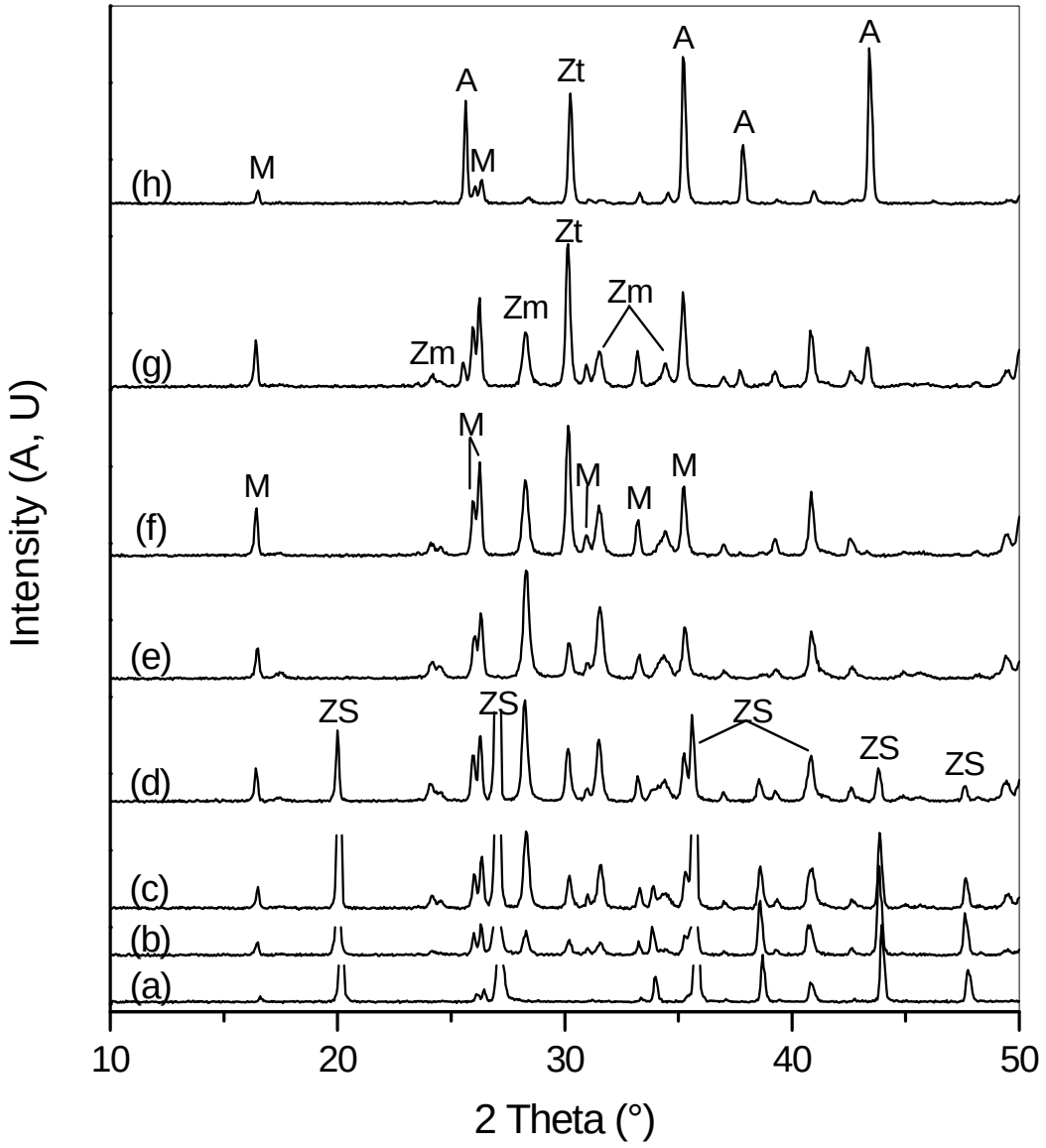

Fig. 1: XRD patterns of various composites heated at 1600°C during 2 hours: M: Mullite, A: Alumina, ZS: Zircon, Zt: Tetragonal-Zirconia and Zm: Monoclinic-Zirconia ; (a) 10%B+90%ZS, (b) 20%B+80%ZS, (c) 30%B+70%ZS, (d) 40%B+60%ZS, (e) 50%B+50%ZS, (f) 60%B+40%ZS, (g) 70%B+30%ZS, (h) 90%B+10%ZS.

located near porous regions. It seems evident that the zirconia's grains transformation was not very sensible to the dilatometric technique used. There was nearly a total absence of hysteresis for 90 wt.% of boehmite. This behavior was attributed to the porous microstructure that absorbs the volume changes of the dispersed particles.

The hysteresis areas do not extend much when the starting powder rate is about 20 or 10 wt.% of boehmite. This hysteresis is not only based on the percentage of zirconia, but also on alumina. The alumina quantity affects the zirconia phase transformation and promotes zircon dissociation. The hysteresis areas are significant for 90 wt.% of zircon.

We believe that the zirconia phase, hysteresis is controlled witness depends not only on the percentage of zirconia, but also that of alumina. The range of temperature to alumina formation is about (1050 - 1100°C). Certain references like sorrel et al. [33] establish that the tetragonal zirconia (Zt) can be contained only in an amorphous matrix. Other authors [34] concluded that the passage of c-ZrO_2/t-ZrO_2 as well as t-ZrO_2/c-ZrO_2 occurred at the expense of the alumina loss. We therefore can assert that the alumina quantity was conditioning the zirconia phase transformation but mullite promotes zircon dissociation. All this incite us to think that alumina promotes formation of composite alumina-zirconia (t), but mullite promotes formation of composite mullite-zirconia (m).

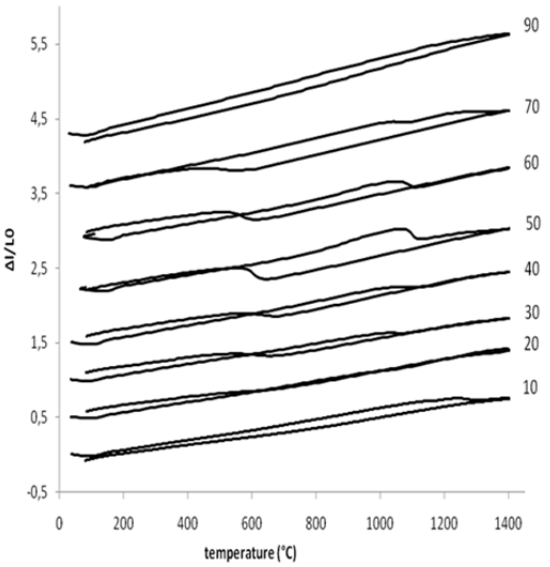

Fig. 2: Dilatometric curves of the composites sintered at 1600°C for 2h.

3.3 Zm-Zt phase transformations

Figure 2 was also used to explore the t/m and m/t phase transformations that occurred during heating and cooling. With these curves, for each composition the temperature at which the transformation occurs, the processing speed as well as the phase transformation duration can be known. The obtained results were grouped in table 2 and table 3 below. Zm/Zt transformation occurs during heating between 970 and 1057°C. Its duration is between 7.33 and 22.49 minutes at a heating rate of 5°C/min. The temperature at the transformations maxima was located between 1007.93°C and 1092.87°C. Its duration takes longer for composite between 40 and 50 wt.% of boehmite, because, there is a large amount of m-ZrO_2 to transform. The processing time decreases out of this interval. At the left side of the interval, the transformation reduction is due to the absence of alumina phase that hosts the t-ZrO_2. At the right side, the processing is reduced by the absence of mullite which is favorable to the formation of monoclinic zirconia.

The reverse Zt/Zm transformation occurred during cooling was slower compared to that occurred during heating. Its transformation speed was about 0.0045 to 0.027 %/min but lasts between 17.49 to 37.47 minutes at a cooling rate of 5°C/min. The temperature for maximal reverse transformations is between 493 and 655°C in relation to the zircons rate increase.

The transformation Zt/Zm occuring during cooling lasts longer than the transformation Zm/Zt occurring during heating because the amount of m-ZrO_2 in the transformation is important in composites with a low rate of boehmite. The temperature intervals were different according to the initial composition of each composite. These results are not in total accordance with the results obtained in references [15, 17] but are closer for the compositions 30 wt.%, 40 wt.% and the 50 wt.% to those cited in the reference [14, 35]. This suggests to us that other factors than the amount of zirconia govern the transformation phenomenon in agreement with Okada's work [16].

The processing temperatures during heating and cooling were affected by many factors such as particle size, impurities and tensions. We did not find in literature how these factors may be involved and their degree of importance. We noticed that the transformation was intense by its duration and its execution speed for the samples containing 40 wt.%, 50 wt.% and 60 wt.% of boehmite. We explain this behavior by the fact that, 50 wt.% and 60 wt.%, of boehmite, corresponds to the maximum amount of zirconia (m and t) which lead us thinking that hysteresis area was proportional to zirconia quantity. Processing speed gradually decreases for other composites. Phase transformation has almost disappeared from the samples containing 10 wt.% of boehmite (low percentages of boehmite) and the samples containing 90 wt.% of boehmite (low percentages of zircon). This was attributed, on the one hand, to the porous microstructure [36] which absorbs the variations of volume of the dispersed particles, and the absence of reactivity due to the insufficient amount of the other powders. These results indicate that the rate of departure are not able to provide an amorphous matrix may contain the monoclinic or tetragonal zirconia which has not been formed or was formed, but in sufficiently small amounts to be detected by dilatometry.

Table 2: Summary table of Zt/Zm transformation rates during heating

Samples	Starting temperature (°C)	Ending temperature (°C)	Temperature Interval (°C)	Duration (min)	Processing speed % /Min	Peak's temperature (°C)
10B/90ZS	-	-	-	-	-	-
20B/80ZS	970.95	1045.94	75.00	15.00	0.0026	1007.93
30B/70ZS	1007.91	1070.38	62.48	12,49	0.0055	1045.39
40B/60ZS	1020.39	1132.86	112.47	22,49	0.0059	1070.37
50B/50ZS	1054.89	1131.11	76.22	15.24	0,0290	1092.87
60B/40ZS	1057.88	1120.34	62.46	12.49	0,0180	1082.85
70B/30ZS	1045.39	1082.02	36.63	07.33	0.0074	1057.88
90B/10ZS	-	-	-	-	-	-

Table 3: Summary table of Zt/Zm transformation rates during cooling

Samples	Starting temperature (°C)	Ending temperature (°C)	Temperature Interval (°C)	Duration (min)	Processing speed % /Min	Peak's temperature (°C)
10B/90ZS	-	-	-	-	-	-
20B/80ZS	643.13	455.78	187,35	37.47	0.0045	593.14
30B/70ZS	655.67	543.20	112.46	22.49	0.0057	605.67
40B/60ZS	677.90	559.75	118.15	23.63	0.0077	655.67
50B/50ZS	633.14	545.66	87.48	17.49	0,0270	608.16
60B/40ZS	618.16	530.70	87.46	17.49	0,0140	568.19
70B/30ZS	568.18	417.39	150.79	30.16	0.0068	493.24
90B/10ZS	-	-	-	-	-	-

3.4 Phase transformation quantification:

Figure 3 shows a comparison between theoretical calculations and results obtained according to Li's work [37] based on XRD analysis on samples sintered at 1600°C. We note a great difference between the theoretical results based on the weight of chemical reactions and quantitative estimates using X-ray spectra according to the equations cited by Li [37]. The amounts of zircon, α-Al_2O_3, mullite and the total ZrO_2 (the sum of tetragonal and monoclinic zirconia) presented in phase ratio are presented in Fig. 3. The results are plotted as a function of starting boehmite percentage. The phase ratio calculated according to theoretical chemical equilibria reaction and that estimated according to Li [37] are shown respectively in figures 3-a and 3-b. The estimated error in the quantitative measurement was ± 3%.

It was found that the histograms were not consistent, especially for zirconia and mullite, beyond 50% of boehmite. The deviations of the quantitative estimates obtained according to reference [37] in comparison with theoretical values and the real results deduced from X-ray spectra can be explained. Li and khor [37] have calculate zirconia rates, only on the basis of peaks of zircon, monoclinic and tetragonal zirconia, without taking into consideration the interactions with alumina and mullite formation.

We provide in the following the equations for estimating the phases rates, considering that all of zircon, monoclinic and tetragonal zirconia, mullite and alumina phases, are present and constitute the composite. The phase ratio of each of them can be estimated by the equations given below:

$$R_{ZrO2(t+m)} = \frac{I_{\{ZrO2-t(111)\}}+I_{\{ZrO2-m(11\bar{1})\}}}{I_{\{ZrSiO4(200)\}}+I_{\{Al2O3(012)\}}+I_{\{mull(210)\}}+I_{\{ZrO2-t(111)\}}+I_{\{ZrO2-m(11\bar{1})\}}} X100\% \quad (12)$$

$$R_{\mathrm{Alumina}} = \frac{I_{\{Al2O3(012)\}}}{I_{\{ZrSiO4(200)\}}+I_{\{Al2O3(012)\}}+I_{\{mull(210)\}}+I_{\{ZrO2-t(111)\}}+I_{\{ZrO2-m(11\bar{1})\}}} X100\% \quad (13)$$

$$R_{\mathrm{mullite}} = \frac{I_{\{mull(210)\}}}{I_{\{ZrSiO4(200)\}}+I_{\{Al2O3(012)\}}+I_{\{mull(210)\}}+I_{\{ZrO2-t(111)\}}+I_{\{ZrO2-m(11\bar{1})\}}} X100\% \quad (14)$$

$$R_{\mathrm{ZrSiO4}} = \frac{I_{\{ZrSiO4(200)\}}}{I_{\{ZrSiO4(200)\}}+I_{\{Al2O3(012)\}}+I_{\{mull(210)\}}+I_{\{ZrO2-t(111)\}}+I_{\{ZrO2-m(11\bar{1})\}}} X100\% \quad (15)$$

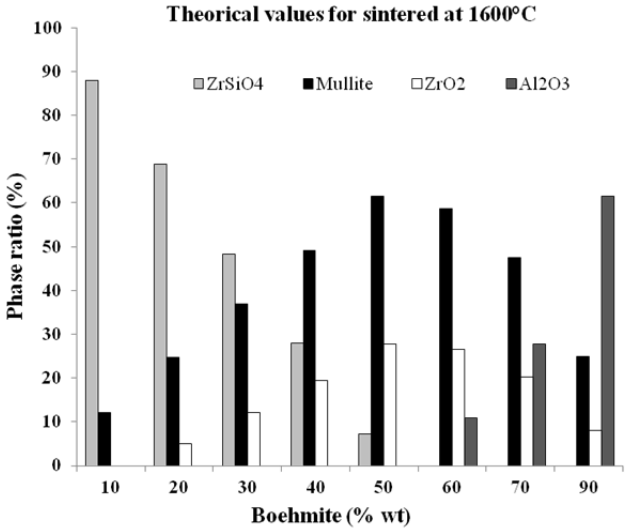

Fig 3-a: Quantitative estimation of phase ratio calculated according to chemical equilibrates reaction.

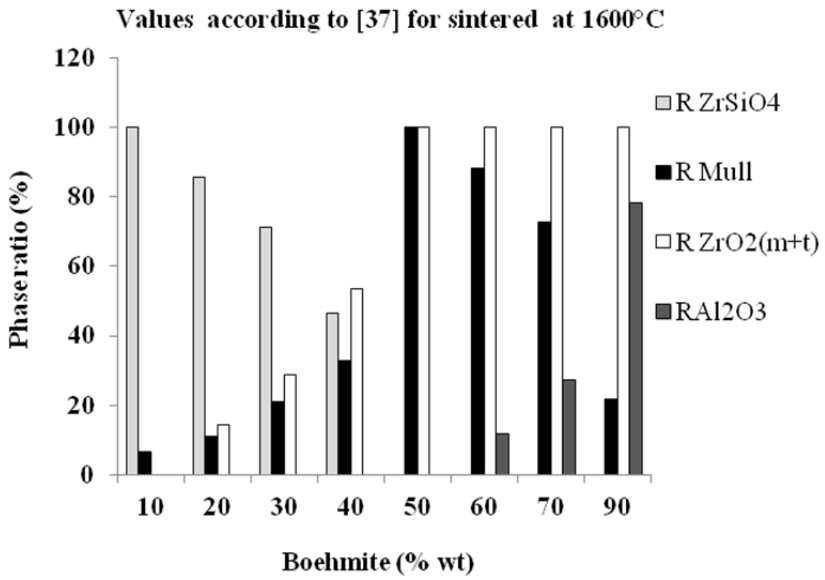

Fig.3-b: Quantitative estimation of phase ratio estimated according to Li and Khor [37].

Empirical corrective coefficients were applied to make the results compatible with the X-rays results. The corrective coefficients 1.686 and 0.35 were assigned respectively for mullite and zirconia. The corrected results are represented in Fig .4 a - 4 e. The quantitative estimation of relative phase proportions was reported in figure 4. The process and the temperature at which thermal dissociation of the zircon starts depends on the presence of impurities. In function of sintering temperature the following remarks can be made:

The formation of mullite is conditioned by the amounts of SiO_2 and Al_2O_3 formed by the zircon's dissociation and the boehmite transformation. In function of temperature and taking in account only the maximal amounts obtained, mullite begin to appear at 1400°C consisting of about 9.8 %, mullite's rate that increases gradually in function of temperature. It reaches 19.3 % at 1450°C, 54.73 % at 1500°C, 57.53 % at 1550°C and 60.88 % at 1600°C. This increase is attributed to zircon's dissociation which activates in function of temperature.

Alumina derived from the processing of the boehmite is consumed for the formation of mullite where the SiO_2 coming from the dissociated zircon is in amounts sufficient to initiate the reaction of the formation of mullite. Therefore alumina appears only when it was in excess. At 1400°C, we note the presence of great quantity of alumina, because it was not reacted with silica in the samples containing 60, 70 and 90 wt.% of boehmite. For composites sintered at 1400°C and 1450°C, the alumina is derived even 20 % of boehmite. This is due to the low starting zircon dissociation at 1450°C.

At 1400°C and 1450°C, the zircon's dissociation is not completed. Alumina issued from boehmite was entirely consumed leading to the formation of mullite in small amounts due to low reactivity between alumina and silica at these temperatures. Depending on the initial ratio of boehmite, we obtained at the end of the treatment the following multi-phase composites:

- Composite of Zircon-Mullite (ZSM) for Lower than 20 wt.% of boehmite
- Composites of Zircon-mullite-alumina (ZSMA) and Zircon-mullite-zirconia-alumina (ZSMZA) for ratios of boehmite between 20 to 50 wt.%.
- Composites of Zircon-alumina-zirconia (ZSAZ) and Zircon-alumina-mullite-zirconia (ZSAMZ) for ratios of boehmite between 60 to 70 wt.%.
- Composite of Alumina-zircon-zirconia (AZSZ) for 90 wt.% of boehmite

At 1500°C, a total decomposition of zircon in the samples containing more than 60 wt.% of boehmite. Depending on the initial boehmite ratio, four composites were obtained:

- Composites of Zircon-mullite (ZSM) for Lower than 20 wt.% of boehmite,
- Composites of Zircon-mullite-zirconia (ZSMZ) for ratios of boehmite between 20 to 40 wt.%,
- Composites of Mullite-zirconia-zircon (MZZS) for 50 wt.% of boehmite,
- Composites of Mullite-zirconia-alumina (MZA) for ratios of boehmite between 50 to 70 wt.%,
- Composites of Alumina-mullite-zirconia (AMZ) for 90 wt.% of boehmite.

For composites sintered at 1550 and 1600°C, the reaction between alumina and zircon was completed and the dissociation of zircon and formation of mullite and zirconia are finished in the samples containing more than of 50 wt.% of boehmite. The following composites were obtained:

- Composites of Zircon-mullite (ZSM) for lower than 20 wt.% of boehmite,
- Composites of Zircon-mullite-zirconia (ZSMZ) and Mullite-zircon-zirconia (MZSZ) for ratios of boehmite between 20 to 40 wt.%,

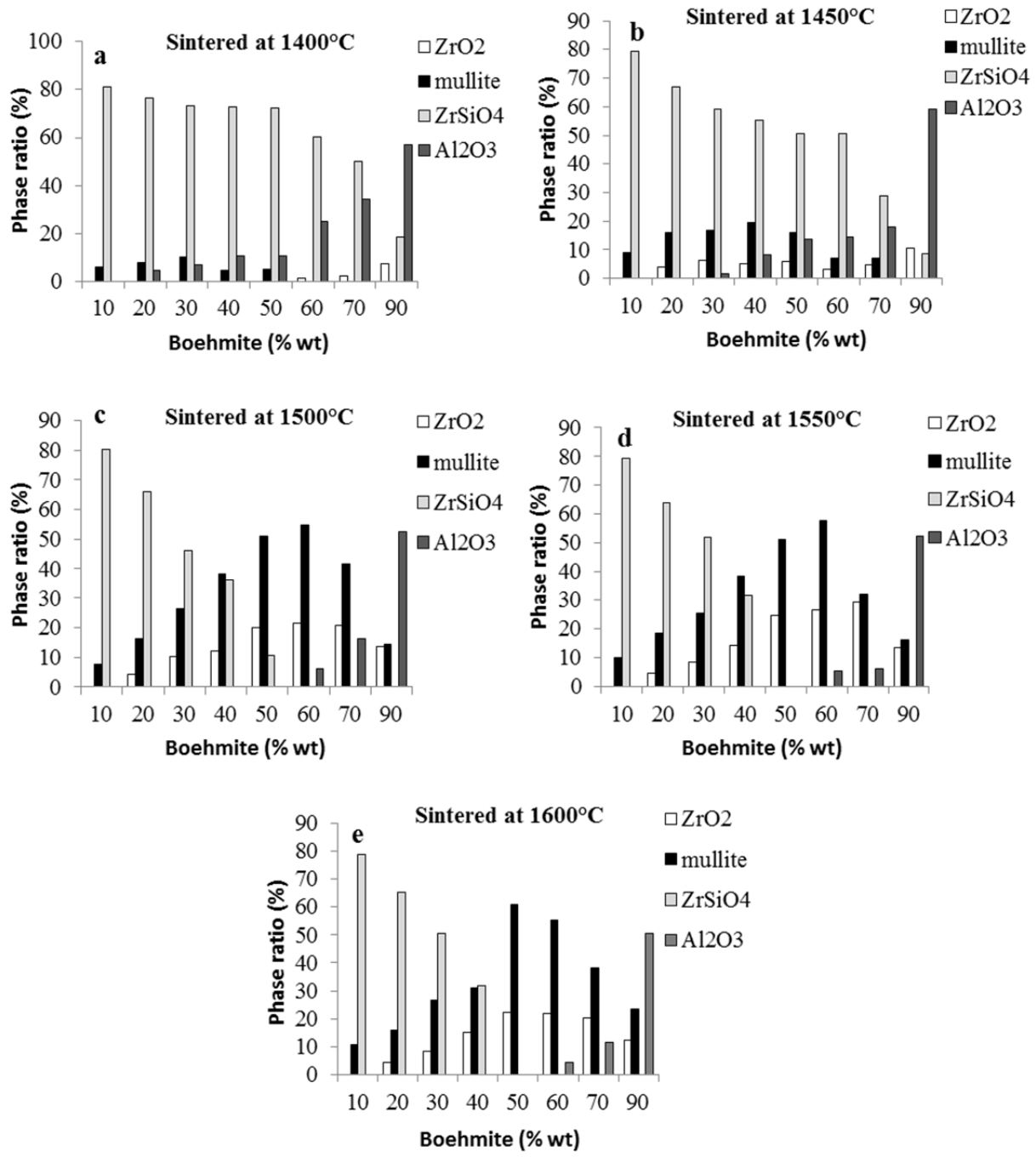

Fig. 4: (a – e) Corrected quantitative estimation of relative phase proportions based on the analysis of XRD data for samples reaction sintered between 1400 and 1600°C.

- Composites of Mullite-zirconia (MZ) for 50 wt% of boehmite,
- Composites of Mullite-zirconia-alumina (MZA) for ratios of boehmite between 60 to 70 wt.% of boehmite,
- Composites of Alumina-mullite-zirconia (AMZ) for 90 wt.% of boehmite.

The zircon dissociation and the relative fraction of zirconia phases formed in different samples are showed in Figure 5 and Figure 6 respectively. We firstly remarked that temperature enormously affects the rate of zircon dissociation. The heating treatment at 1400°C is too low to cause dissociation of zircon. At 1450°C, the dissociation rate was very slow and was not total. The dissociation of zircon is enhanced by addition of boehmite (> 50 wt.% of boehmite). For samples sintered at 1550 and 1600°C, the dissociation of zircon is completed from 50 wt.% of boehmite. For those sintered at 1500°C, a total dissociation was observed from 60 wt.% of boehmite. The relative fraction of monoclinic and tetragonal zirconia phases in function of initial boehmite rate, are shown in figure 7 and 8 relatively. A temperature of 1500°C must be reached at least to obtain formation of a good amount of zirconia. The m-ZrO_2 relative fraction increases with high zircon content whereas the t-ZrO_2 fraction increases with boehmite

rate growth. A partial thermal dissociation of zircon when boehmite was in low proportions leads to zirconia monoclinic. This was attributed to the presence of the mullite for these concentrations which promote the m-ZrO_2 formation. For composites made with 70 and 90 wt.% of boehmite, the zirconia formed, was almost tetragonal. This can be explained by the fact that alumina promotes the formation of t-ZrO_2. The formation of Zt had started only from 50 wt.% for low rate of boehmite at 1400°C. It increases rapidly beyond this rate.

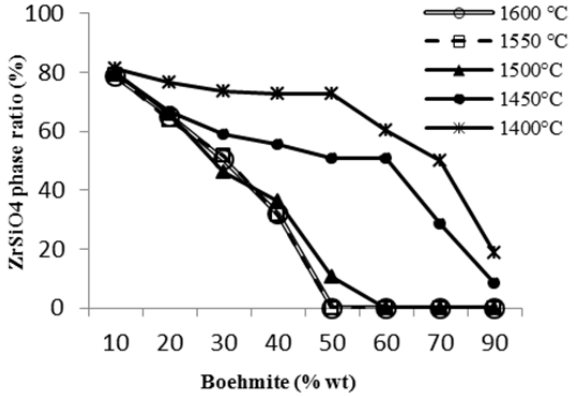

Fig. 5: Zircon fraction in reaction sintered samples at different temperatures.

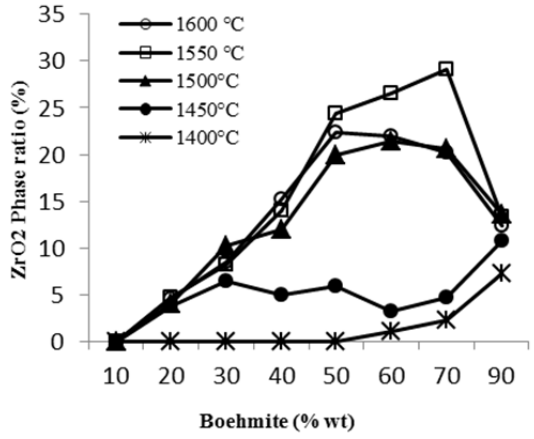

Fig. 6: Total zirconia formation in reaction sintered samples at different temperatures.

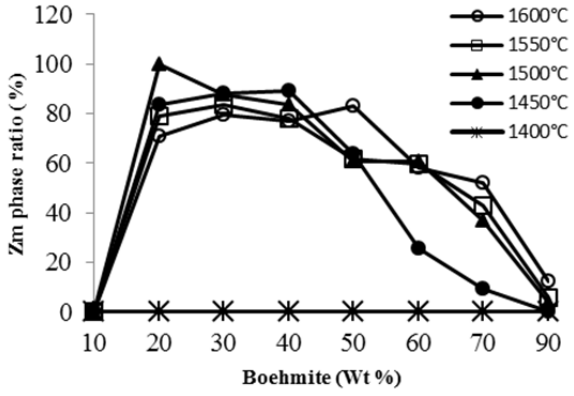

Fig. 7: Monoclinic zirconia fraction in reaction sintered samples at different temperatures.

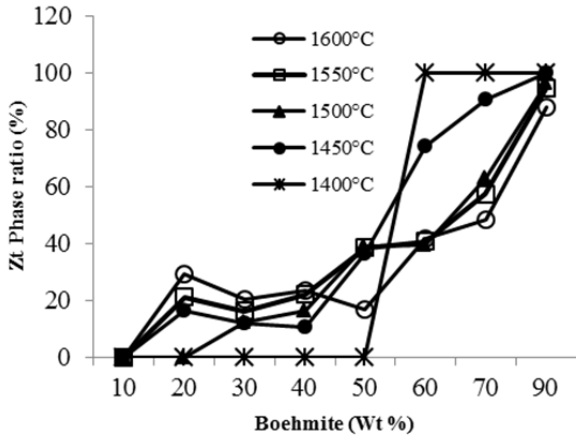

Fig. 8: Tetragonal zirconia fraction in reaction sintered samples at different temperatures.

3.5 Mechanical properties characterization

The variations of the micro hardness (Hv), Young modulus (E) and the toughness (K_{IC}) with the initial content of boehmite are shown in Figure 9. We notice that the curves of Hv and E vary in the same way. There is a sharp decrease in Hv and E values around of 20 and 40 wt.% of boehmite followed by an important increase up to 70 wt.% of boehmite, followed by another increase with a different slope. We can associate these variations of the mechanical properties by the structure obtained and by the amount of phases in presence. In the vicinity of 10 wt.% of boehmite, it was normal that values of E = 225 GPa and Hv = 14 GP are reached. These values are close to values of zircon which is the dominant phase at this composition. We attribute this decrease to the presence of zirconia resulting from the dissociation of zircon (the sum of tetragonal and monoclinic zirconia) which was in gradual increase and contributes to the micro-cracks connections, and thus significantly reduces the mechanical properties of the composites. A minimum was observed (E = 215 GPa, and Hv = 11.5 to 12 GPa), for samples containing 20 and 40 wt.% of boehmite. This coincides perfectly with the zirconia maximum observed in these samples (figure 7 and figure 8).

Beyond 40 wt.% of boehmite, Hv curves resume their gradual growth up to 90 wt.% of boehmite where Hv is 18.6 GPa. This is due to the gradual growth of alumina phase which enhances the microhardness. Young's modulus (E) curves show a gradual growth between 40 and 60 wt.% of boehmite. The increase of young modulus is attributed to the enrichment by alumina. Beyond 90 wt.% of boehmite it reaches a maximum of 238 GPa with a little change in curve slope. A slight reduction in density was also observed due to the increase of the content of t-ZrO_2 that enriches the monoclinic zirconia produced subsequently. The mechanical properties of zirconia, being substantially less than that of alumina, explain the fact that these properties decrease with increasing zirconia content. Most of the ZrO_2 formed in this composite was monoclinic.

From the general shape of the curves, it appears that composites with m-ZrO_2 had weaker mechanical properties than those of composites with t-ZrO_2. The presence of tetragonal zirconia increases strength by transformation toughening of the composites [37]. The presence of t-ZrO_2 and m-ZrO_2, as second phases, both contribute to the improvement of mechanical properties and strengthening and improving the microstructure. The latter, which is itself a type of reinforcement, has a lesser effect. Measurements of elastic modulus are useful in so far as they tell us about the condition of the interior of the composite.

A several variations in the slope of the toughness curve (K_{IC}) were remarked. The toughness values obtained for the composites with high m-ZrO_2 rate are the highest. K_{IC} reaches its high values 4.74 MPa.$m^{1/2}$ for the zircon-mullite (ZSM) composites, obtained for the samples containing 20 wt.% of boehmite, due to high zircon content. K_{IC} decreases a bit down to 4.28 and 4.07 MPa.$m^{1/2}$ for the mullite-zirconia (MZ) composites containing 50 and 60 wt.% of boehmite respectively. A noticeable decrease was observed 3.65 MPa.$m^{1/2}$ in samples containing 90 wt.% of boehmite, which corresponds to the appearance to Zt and the formation of alumina-zirconia-mullite (AZM) composites.

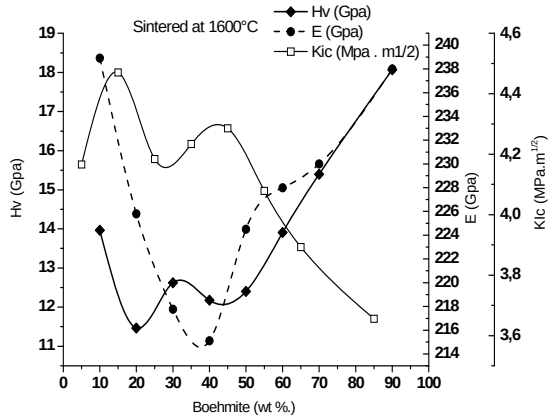

Fig. 9: Microhardness (Hv), young's modulus (E) and toughness (K_{IC}) as a function of boehmite content.

Typical observed Vickers indentation is shown in figure 10. Well-shaped indentations with median-radial cracks propagating from the corners of the imprints were obtained. There is no development of lateral cracks in contact. This may be attributed to the mechanism which absorbs cracks energy like development of microcracks caused by anisotropies of different phases and porosity. SEM micrographs of indentation print at lower indentation load of 15 N for composites sintered at 1600°C are shown in Fig. 11. Considering the crack propagation path, the main fracture mode assumed in these materials is mixture, intragranular and intergranular. The continuous straight of crack path observed with no evidence of deflection or bridging indicates that the crack propagates in the same way through the zircon and mullite grains. This suggests there is a good cohesion between mullite and zirconia grains. Toughening mechanisms such as transformation toughening or crack bridging and deflection are clearly not operative in our material.

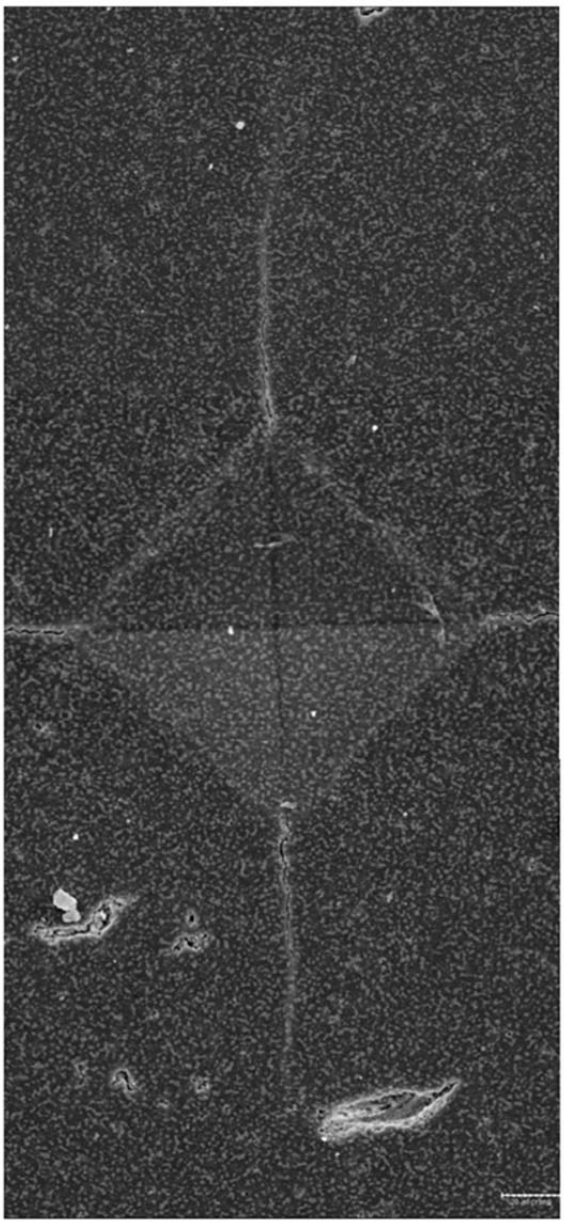

Fig. 10: Vickers impression and radial cracks in composite 60 wt.% sintered at 1600°C, 2h (bar = 20 microns).

The structure of the sample containing 60 wt.% of boehmite and sintered at 1600°C is biphasic. It is composed of large grains of mullite and particles of intergranular and intragranular zirconia.

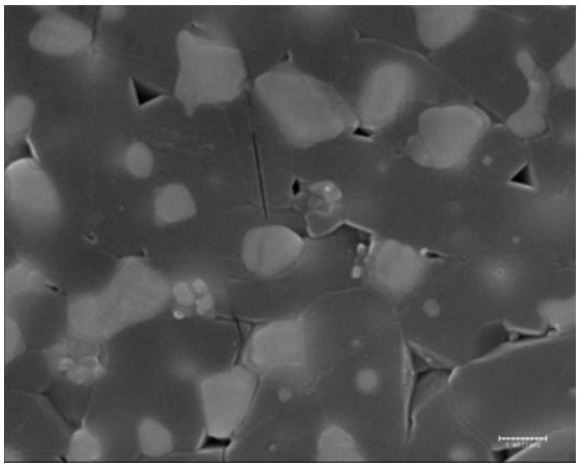

Fig. 11: SEM micrograph showing indentation crack propagation in composite containing 60 wt% of boehmite sintered at 1600°C, 2h (bar =1micron).

The intergranular zirconia elongated and a random shape, while the intragranular zirconia with spherical shape and relatively lower size.

3.6 Linear expansion coefficient

Values of the expansion coefficient for each composite during heating between 200°C and 600°C are represented in figure 12.

Zirconia has the highest coefficient of thermal expansion (10×10^{-6} K^{-1}) compared to alumina (8.2×10^{-6} K^{-1}), mullite (5.3×10^{-6} K^{-1}) and Zircon (4.5×10^{-6} K^{-1}). They do not differ significantly as expected, since the thermal expansion coefficient increasing rate, depends on the zirconia content. The curve showed several variation phases of the expansion coefficient: a slow growth with increasing percentage of boehmite, below 40 wt.% followed by a small decrease up to 50 wt.% before increasing again slowly and then sharply beyond 60 wt.%. We can associate these variations to the structure obtained. In the case where the zircon was in excess relatively to boehmite we have mullite-zirconia composites with an excess of remaining zircon that contributes to a thermal expansion decrease. The tendency to the growth of the curve below 40 wt.% of boehmite was associated with the disappearance of zircon as alumina rate increases. This latter was reacting to constitute more of mullite and zirconia. It was estimated that the increasing alumina rate contributed to the recording of the peak for the 40 wt.% of boehmite.

The minimum of the expansion coefficient was observed in the sample containing 50 wt.% of boehmite, corresponds to the presence of mullite which has a tendency for low dilatation in addition to the loss of the entire zirconia which was used. The curve recovers its growth with increasing alumina coming from boehmite but the values remains weak and close to those of the mullite coefficient. The composites matrix is mullitic with small quantities of alumina and zircon.

These latter are gradually declining contributing to the lowering of the zirconia rate which in turn influences on the dilatation coefficient. The growth noticed in the sample containing 60 wt.% of boehmite corresponds to the effect of the alumina coming from boehmite excess. This alpha alumina is associated with the small amount of zirconia forming the mullite-alumina-zirconia (MAZ) composites with an excess of alumina which lead to a notable increase of the expansion thermal coefficient.

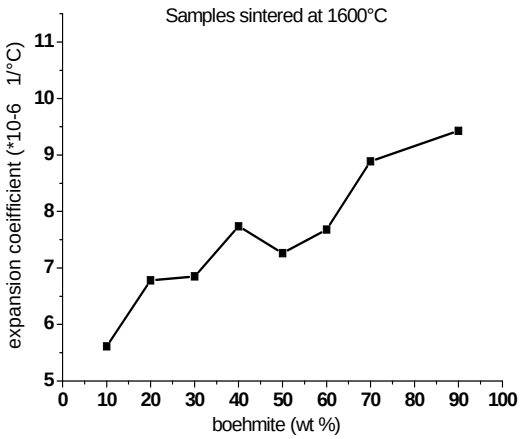

Fig. 12: The coefficient of expansion evolution as a function of the composition.

4. CONCLUSION

This study demonstrates the possibility to produce multiphase composites from a mixture of only two powders; boehmite and zircon (materials which are easy to obtain), without additives or stabilizers, and proceeding by reaction sintering. It is a very economical way to get a variety of materials.

The phases quantification based on X-ray diffraction spectrograms as described by references cited above, is reliable (with negligible errors) in the case of composites with low boehmite rate (below 50 wt.%). Beyond this rate, this technique becomes unreliable for zirconia and mullite phases. We proposed for those cases some rectifications on the quantification equations by affecting corrective coefficients (0.35 for zirconia and 1.686 for mullite).

The low hysteresis area or the absence of transformation's hysteresis is attributed on one hand to the lack of the zirconia quantity attributed to insufficient of zircon and the boehmite which reacts on the other hand. The microstructure which is very porous tends to absorb any changes in the volume of dispersed particles.

We observed that the mechanical properties of the composites prepared by such materials and processing technique are rather satisfactory in comparison with similar works cited in literature.

REFERENCES

1. **K. A. Khor and Y. Li**, Effects of mechanical alloying on the reaction sintering of ZrSiO4 and Al_2O_3. Materials Science and Engineering A256, (1998), 271-279.
2. **N. Claussen and J. Jahn,** Mechanical properties of sintered, in situ reacted mullite-zirconia composites, J. Am. Ceram. Soc., Vol. [**63**], 3-4, (1980), 228-229.
3. **J. S. Moya and M. I. Osendi**, Microstructure and mechanical properties of mullite/ZrO_2 composites, J. Mater. Sci., Vol. [**19**], (1984), 2909-2914.
4. **M. Awaad, M. F. Zawrah and N.M. Khalil**, In situ formation of zirconia-alumina-spinel-mullite ceramic composites, Ceram. Inter., Vol. [**34**], (2008), 429-434.
5. **G. Orange, G. Fantozzi, F. Cambier, C. Leblud, M. R. Anseau and A. Leriche**, High temperature mechanical properties of reaction-sintered mullite/zirconia and mullite/alumina/zirconia composites, Journal of Materials Science, Vol. [**20**], (1985), 2533-2540.
6. **G. M. Asmelash, O. Mamat and F. Ahmad**, Toughening mechanisms of Al_2O_3-SiO_2-ZrO_2 composite materials, Ceramics Silikáty, Vol. [**56**], 4, (2012), 360-366.
7. **N. M. Rendtorff, L. B. Garrido and E. F. Aglietti**, Mechanical and fracture properties of zircon-mullite composites obtained by direct sintering, Ceram. Inter., Vol. [**35**], (2009), 2907-2913.
8. **E. D. Rupo and M. R. Anseau**, Solid state reactions in the ZrO_2-SiO_2-αAl_2O_3 system, Journal of materials science, Vol. [**15**], (1980), 114-118.
9. **C. Aksel**, Mechanical properties and thermal shock behaviour of alumina-mullite-zirconia and alumina-mullite refractory materials by slip casting, Ceram. Inter., Vol. [**29**], (2003), 311-316.
10. **Q. L. Ge, T. C. Lei, J. F. Mao and Y. Zhou**, In situ transmission electron microscopy observations of the tetragonal to monoclinic phase transformation of zirconia in Al_2O_3-ZrO_2 (2 mol % Y_2O_3) composite, Journal of materials science letters, Vol. [**12**], (1993) 819-822.
11. **J. Zhong, J. Zhao, S. Liang, X. Tan, M. Zhou and G. Zhang**, Synthesis of spherical (30 nm) and rod-like (200 nm) zirconia co-reinforced mullite nanocomposites, Ceram. Inter., Vol. [**39**], (2013), 4163-4170.
12. **H. M. Jang, S. M. Cho and K. T. Kim**, Alumina-mullite-zirconia composites, Part 1 Colloidal processing and phase-formation characteristics, Journal of materials science, Vol. [**31**], (1996), 5083-5092.
13. **B. Basu, J. Vleugels and O. Van Der Biest**, Transformation behaviour of tetragonal zirconia: role of dopant content and distribution, Materials Science and Engineering A366, (2004), 338-347.
14. **M. Hamidouche, N. Bouaouadja, H. Osmani, R. Torrecilas and G. Fantozzi**, Thermomechanical behaviour of mullite zirconia composite, J. Eur. Ceram. Soc., Vol. [**35**], (1996), 441-445.
15. **N. M. Rendtorff, L. B. Garrido and E. F. Aglietti**, Thermal behavior of mullite-zirconia-zircon composites. Influence of zirconia phase transformation, J. Therm. Anal. Calorim., Vol. [**104**], (2011), 569-576.
16. **H. Okada, T. Tamura, N. Ramakrishnan, S. N. Atluri and J. S. Epstein**, Analysis of toughening of magnesia partially stabilized zirconia, due to dilatational transformation, Acta. Metal. Mater., Vol. [**40**], 6, (1992), 1421-1432.
17. **S. Riou, F. Queyroux and P. Boch**, Zirconia-alumina particulate composites by infiltration processing, Ceram. Inter., Vol. [**21**], (1995), 339-343.
18. **R. C. Garvie and P. S. Nicholson**, Phase analysis in zirconia systems, J. Am. Ceram. Soc., Vol. [**55**], 6, (1972), 303-305.
19. **Y. Li and K. A. Khor**, Microstructure and composition analysis in plasma sprayed coatings of Al_2O_3-$ZrSiO_4$ mixtures, Surface and Coatings Technology, Vol. [**150**], (2002), 125-132.
20. **H. K. Schmid**, Quantitative analysis of polymorphic mixes of zirconia by X-ray diffraction, J. Am. Ceram. Soc., Vol. [**70**], (1987), 367-376.
21. **G. L. Leatherman and M. Tomozawa**, Mechanical properties of a transformation toughened glass-ceramic, J. Mater. Sci., Vol. [**25**], (1990), 4488-4494.
22. **P. Miranzo, P. Pena, J. S. Moya, S. De Aza**, Multicomponent toughened ceramic materials obtained by reaction sintering. Part 2 System ZrO_2-Al_2O_3-SiO_2-MgO, J. Mater. Sci., Vol. [**20**], (1985), 2702-2710.
23. **T. Koyama, S. Hayashi, A. Yasumori, K. Okada, M. Schmucker and H. Schneider**, Microstructure and mechanical properties of mullite/zirconia composites prepared from alumina and zircon under various firing conditions, J. Eur. Ceram. Soc., Vol. [**16**], (1996), 231-237.
24. **A. C. Mazzei and J. A. Rodrigues**, Alumina-mullite-zirconia composites obtained by reaction sintering. Part I Microstructure and mechanical behaviour, J. Mater. Sci., Vol. [**35**], (2000), 2807-2814.
25. **L. B. Garrido and E. F. Aglietti**, Reaction-sintered mullite-zirconia composites by colloidal processing of alumina-zircon-CeO_2 mixtures, Materials Science and Engineering A369, (2004), 250-257.
26. **K. A. Khor, L. G. Yu, Y. Li, Z. L. Dong and Z. A. Munir**, Spark plasma reaction sintering of ZrO_2/mullite composites from plasma spheroidized zircon/alumina powders, Materials Science and Engineering A339, (2003), 286-296.

27. **E. Rocha-Rangel, S. Diaz-De-La-Torre, M. Sumemoto and H. Miyamoto**, Zirconia-mullite composites consolidated by spark plasma reaction sintering from zircon and alumina, J. Am. Ceram. Soc., Vol. [**88**], 5, (2005), 1150-1157.
28. **P. Pena, P. Miranzo, J. S. Moya and S. De Aza**, Multicomponent toughened ceramic materials obtained by reaction sintering. Part 1 ZrO_2-Al_2O_3-SiO_2-CaO system, Journal of materials science, Vol. [**20**], (1985), 2011-2022.
29. **S. Liang, J. Zhong, X. Tan and Y. Tand**, Mechanical properties and structure of zirconia-mullite ceramics prepared by in-situ controlled crystallization of Si-Al-Zr-O amorphous bulk, Trans. Nonferrous Met. Soc. China, Vol. [**18**], (2008), 799-803.
30. **G. R. Anstis, P. Chantiklul, B. R. Lawn and D. B. Marshall**, A critical evaluation of indentation techniques for measuring fracture toughness: I, Direct crack measurements, J. Am. Ceram. Soc., Vol. [**64**], 9, (1981), 533-538.
31. **D. Casellas, N. M. Nagl, et al.,** Growth of Surface Indentation Cracks in Alumina and Zirconia Toughened Alumina, Key Engineering Materials, Vol. [**127-131**], (1997), 895-902.
32. M. **Hamidouche, N. Bouaouadja, R. Torrecillas and G. Fantozzi**, Thermomechanical behavior of a zircon–mullite composite, Ceram. Inter., Vol. [**33**], (2007), 655-662.
33. **C. A. Sorrel and C. C. Sorrel,** Subsolidus Equilibria and Stabilization of Tetragonal ZrO_2 in the System ZrO_2-Al_2O_3-SiO_2, J. Am. Ceram. Soc., Vol. [**60**], 11-12, (1977), 495-499.
34. **L. Gao, Q, Liu, J. S. Hong, H. Miyamoto, S. D. Delatorre, A. Kakitsuji, K. Liddel and D. P. Thompson**, Phase transformation in the Al_2O_3-ZrO_2 system, Journal of materials science, Vol. [**33**], (1998), 1399-1403.
35. **W. H. Tuan, R. Z. Chent, C. Wang, C. H. Cheng and P. S. Kuo**, Mechanical properties of Al_2O_3/ZrO_2 composites, J. Eur. Ceram. Soc., Vol. [**22**], (2002), 2827-2833.
36. **H. Belhouchet, H. Makri, M. Hamidouche, N. Bouaouadja, V. Garnier and G. Fantozzi**, Elaboration and characterization of multiphase composites obtained by reaction sintering of boehmite and zircon, J. Aust. Ceram. Soc., Vol. [**50**], 2, (2014), 135-146.
37. **Y. Li and K.A. Khor,** A Study of Processing Parameters in Thermal-Sprayed Alumina and Zircon Mixtures, Journal of Thermal Spray Technology, Vol. [**11**], 2, (2002), 186-194.